Multistage Single Clad 2µm TDFA with a Shared L-Band Pump Source

Robert E. Tench [a], Clément Romano [a,b], and Jean-Marc Delavaux [a]

[a] Cybel LLC, 1195 Pennsylvania Avenue, Bethlehem, PA 18018 USA
[b] Institut Telecom/Telecom ParisTech, 46 Rue Barrault, 75634, Paris France
robert.tench@cybel-llc.com

Abstract

We report the experimental performance and simulation of a multiwatt two-stage TDFA using an L-band (1567 nm) shared pump source. We focus on the behavior of the amplifier for the parameters of output power P_{out}, gain G, noise figure NF, signal wavelength λ_s, and dynamic range. We measure the spectral performance of the TDFA for three specific wavelengths (λ_s= 1909, 1952, and 2004 nm) chosen to cover the low-, mid-, and upper-wavelength operating regions of the wideband amplifier. We also compare the performance of the two-stage shared pump TDFA with a one stage shared pump amplifier. Experimental results are in good agreement with simulation.

1. Introduction

The broad bandwidth of single clad Thulium-doped fiber amplifiers (SC-TDFAs) has been demonstrated for different wavelength bands, in applications ranging from spectral sensing and LIDAR to high energy physics and telecommunications. Design optimization of amplifier architecture is critical for the practical realization of wideband, compact, and efficient TDFAs for these applications. Recently, we have reported results showing that single clad TDFAs can provide a combination of large gain and high output power over extended bandwidths [1-4]. In this work, we investigate the optimization of tandem single clad amplifier topologies for wideband TDFAs. In particular we focus on the simulation and experimental performance of a tandem (two-stage) single clad TDFA using an L-band (1567 nm) shared fiber laser pump source. We highlight the amplifier performance in the key areas of high output power (> 2W), high gain (> 60 dB), low noise figure (< 3.5 dB), and large dynamic range (> 35 dB.) We also evaluate the wavelength behavior of the SC-TDFA by measuring its performance at three specific wavelengths (1909, 1952, and 2004 nm) which are chosen to cover the low-, mid-, and upper-wavelength operating regions of the amplifier spectral response. We then contrast the performance of our tandem amplifier with that of recent single stage SC-TDFAs. In comparing the topologies, we illustrate and discuss the tradeoffs for optimizing the TDFA configuration in a specific operating band.

The paper is organized as follows: Section 2 presents our experimental setup, a two stage TDFA with a fixed pump coupling ratio between co-pumping and counter-pumping in the active fibers. Section 3 covers the dependence of experimental amplifier performance on signal input power, total pump power, and signal wavelength. Section 4 compares measurement and simulation of the TDFA performance. Section 5 contrasts our simple TDFA design with performance of a one stage, shared pump design in [4]. Finally, Section 6 discusses design parameter tradeoffs for different TDFA architectures and applications.

2. Experimental Setup for the Shared Pump Amplifier

The optical design of our two-stage single pump TDFA is shown in Figure 1. A single frequency 2 µm DML input source (Eblana Photonics) is coupled through I1 and WDM1 into the active fiber F1. Pump light from a multi-watt fiber laser P1 at 1567 nm is split by coupler C1 with a coupling ratio of 30%/70%. The two pump

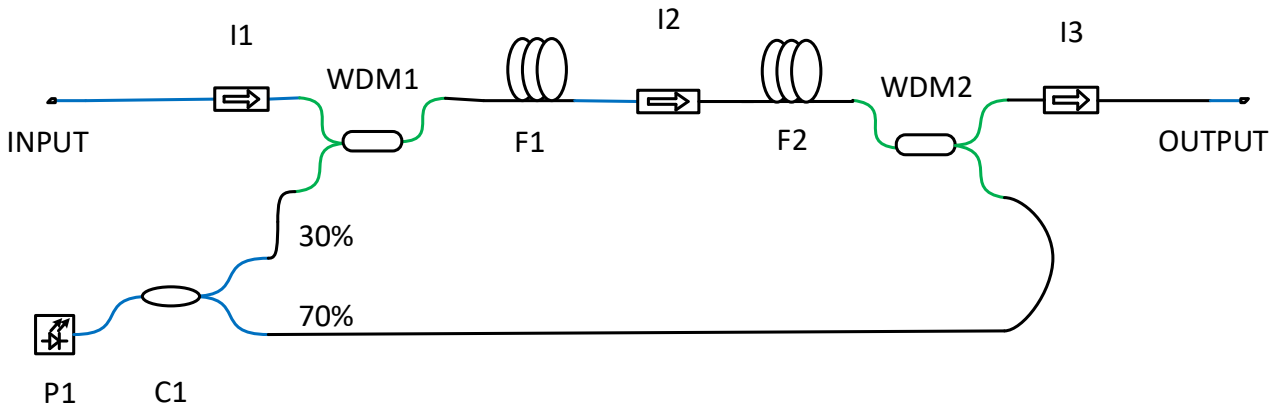

Figure 1. Optical Design of Two Stage Single Pump TDFA with a Shared Pump Arrangement.

WDM = Wavelength Division Multiplexer.

signals co-pump fiber F1 (30%) and counter-pump fiber F2 (70%), respectively. The signal output of F1 is coupled through I2 into F2, and the signal output of F2 then passes to the output through WDM2 and I3. Isolators I1 -I3 ensure unidirectional operation and suppress backward ASE. F1 is 4.3 meters and F2 is 2.0 meters of IXBlue Tm-doped single clad silica fiber (IXF-TDF-4-125-v1). Input and output signal powers, and co-pump and counter-pump powers, are respectively referenced to the inputs and outputs of F1 and F2 (internal gain, power, and noise figure measurements.) Optical power and optical spectra were measured with a Yokogawa AQ6375B optical spectrum analyzer.

3. Experimental Amplifier Performance

The first plot of experimental amplifier performance is in Figure 2, which shows the variation in output power P_{out} as a function of total pump power P_p for various levels of signal input power P_s at a signal wavelength λ_s of 1952 nm. For the maximum P_s of 1.6 dBm, P_{out} = 1.82 W at a total P_p of 3.61 W. The slope efficiency η for this input power, defined as $\eta = \Delta P_{out}/\Delta P_p$, is 54.2 %. This slope efficiency is for the total amplifier, that is, for the total performance of Stage 1 + Stage 2. The optical-optical power conversion efficiency at this point is 1.82 W/3.61 W = 50.4 %. The difference between slope efficiency η and optical-optical power conversion efficiency is caused by the zero crossing or threshold of the output power curve, which crosses the P_{out} axis at a pump power of $\approx$ 0.28 W. Because of this threshold, the slope efficiency η can be significantly greater than the optical-optical power conversion efficiency.

Figure 3 plots the evolution of gain G as a function of P_p for various levels of P_s at 1952 nm. The gain G is defined in the following way:

$$G(\lambda_s) = P_{out}(\lambda_s)/P_s(\lambda_s) \quad (1)$$

Note that G increases with increasing P_p, as expected, and that the maximum gain observed for P_s = -35 dBm is 56.9 dB. For P_p = 3.61 W, the 15 dB gain saturation point occurs for $P_s \approx$ -9 dBm. We note that G = 50 dB can be achieved for a pump power of only 1.2 W, illustrating the high gain performance of the TDFA for low pump powers.

Having established baselines for amplifier performance at λ_s= 1952 nm, we next investigate G and the noise figure NF as a function of signal wavelength.

For these studies, NF is defined by Equations 2-4, using the optical method of measurement [5,6]:

$$N_{eq}(\lambda) = P_{ASE}(\text{forward}, \lambda_s) / (2\ h\ c^2\ \Delta\lambda / \lambda_s^{\ 3})\ G(\lambda_s) \quad (2)$$

$$F(\lambda_s) = (1/ G(\lambda_s)) + 2\ N_{eq}(\lambda_s) \quad (3)$$

$$NF\ (dB) = 10 \log_{10}(F(\lambda_s)) \quad (4)$$

Here P_{ASE} (forward, λ_s) is the forward amplified spontaneous emission power from the output of the TDFA measured in the resolution bandwidth $\Delta\lambda$ of the OSA, h is Planck's constant, and c is the speed of light in vacuum. $G(\lambda_s)$ is defined in Equation 1.

The evolution of G and NF for P_p = 3.61 W is plotted in Figure 4 for the three experimental signal wavelengths of λs = 1909, 1952, and 2004 nm. We first note that G is maximum for 1909 nm and P_s = -35 dBm at 60.4 dB, decreasing to 56.9 dB at 1952 nm and 41.6 dB at 2004 nm. The 15 dB compression points are -13.5 dBm for 1909 nm, -12 dBm for 1952 nm, and ≈ + 6 dBm for 2004 nm. We also observe that small signal NF values are between 3 and 4 dB for all signal wavelengths, rising to 4-5.8 dB for $P_s \approx 2$ dBm. The dynamic range of the amplifier is therefore 38 dB, for the criterion of NF < 5.8 dB. The noise figure over the total dynamic range is within 3 dB of the quantum limit of 3.0 dB, an important factor for telecommunications applications such as in-line amplifiers (repeaters) and optical preamplifiers for receivers.

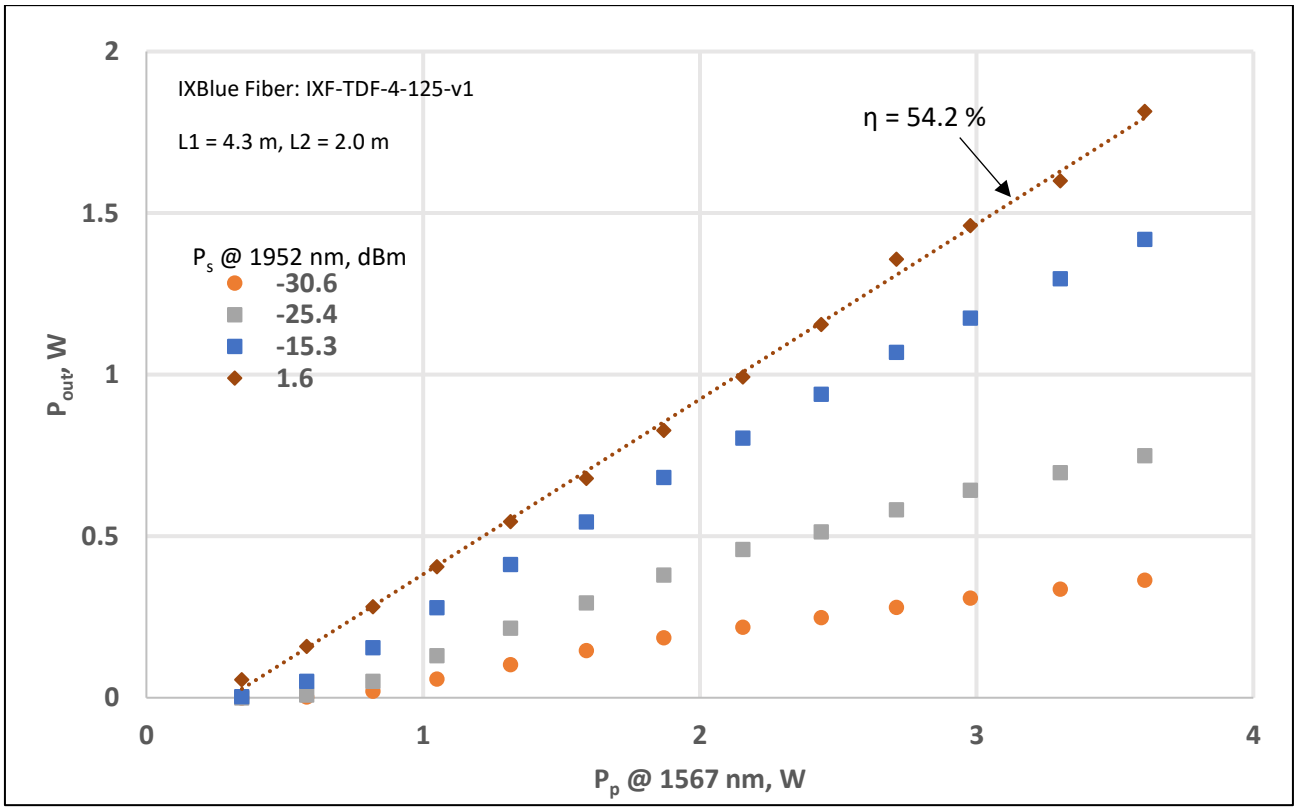

Figure 2. P_{out} vs. P_p for the Parameter of P_s, at 1952 nm. Points: data. Dashed line: linear fit to data.

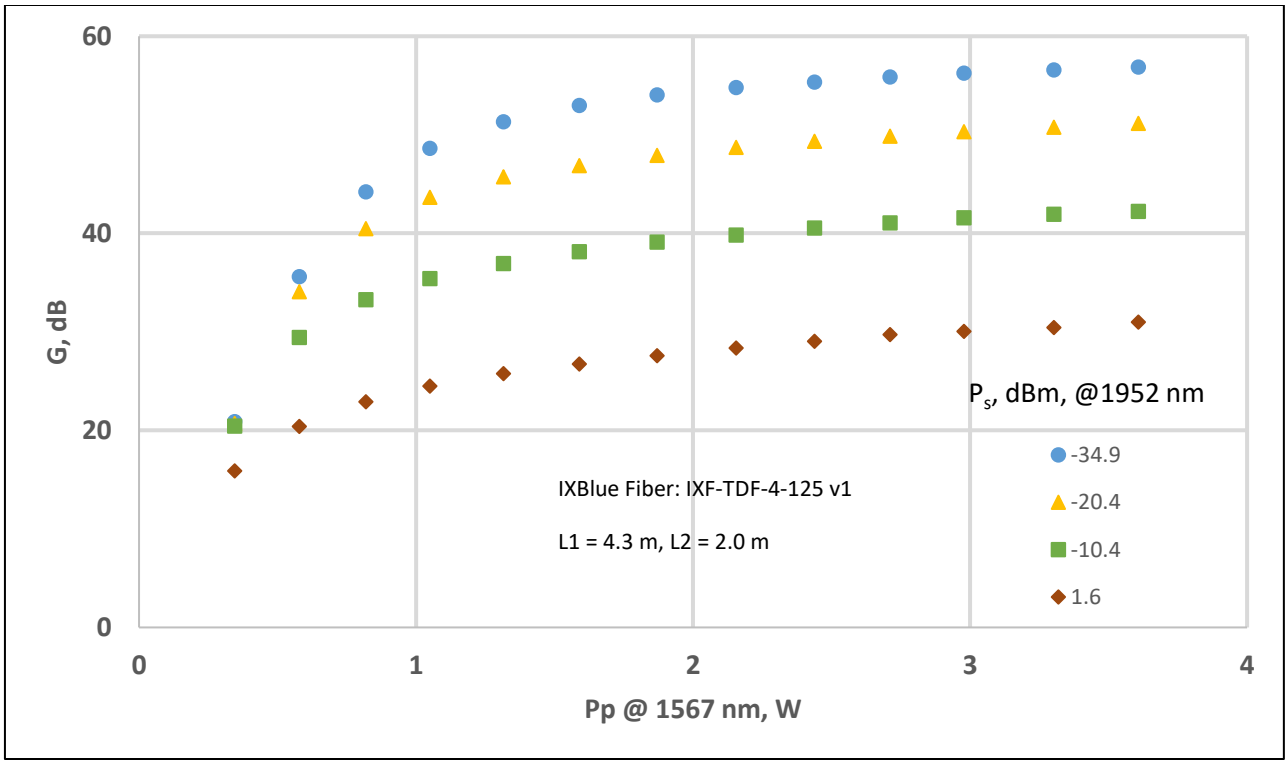

Figure 3. G vs. P_p for the Parameter of P_s, at 1952 nm.

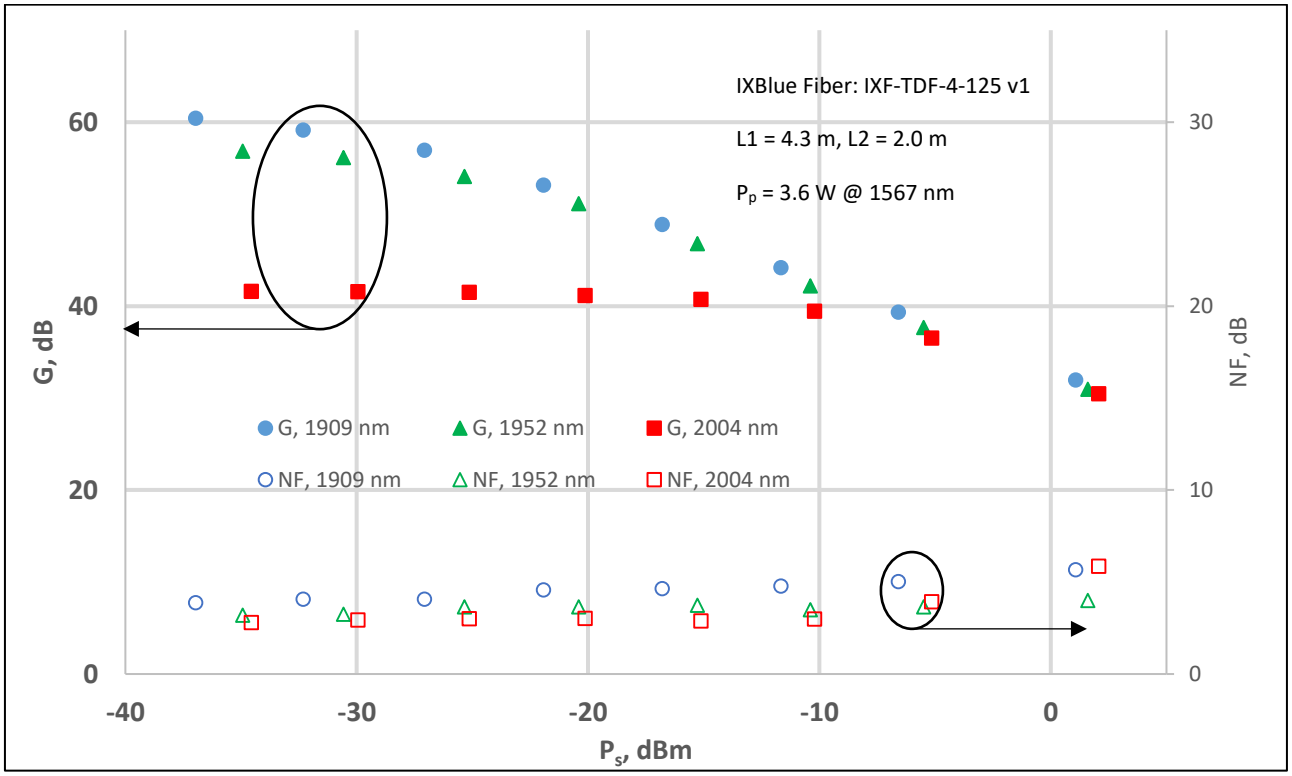

Figure 4. G and NF vs. P_s for P_p = 3.61 W, at 1909, 1952, and 2004 nm.

A graph of P_{out} vs. P_p for the three signal wavelengths studied is shown in Figure 5, for $P_s \approx 1$ dBm. The maximum optical-optical conversion efficiencies are 56.2 % for 1909 nm, 50.4% for 1952 nm, and 50.2 % for 2004 nm. This plot illustrates a key behavior of the two stage TDFA: variations in saturated output power for the amplifier as a function of signal wavelength are relatively small, and high output powers of 1.8 – 2 W can be achieved over the ≈ 100 nm range of measured signal wavelengths.

A plot of slope efficiency η vs. P_s for the three signal wavelengths studied is given in Figure 6. Maximum slope efficiencies are 62.3% for 1909 nm, 54.2 % for 1952 nm, and 55.0% for 2004 nm. The evolution of the slope efficiency curves is quite different for 1909 and 1952 nm compared to 2004 nm. We observe that operation at the long wavelength of 2004 nm requires high input power to obtain a high power conversion efficiency. This behavior is attributed to the variation in the amplifier saturation power as a function of signal wavelength [5] and will be studied further in a future publication.

No nonlinear effects, such as stimulated Brillouin scattering or stimulated Raman scattering, were observed in any of our measurements on the two stage TDFA. This behavior is consistent with calculations of nonlinear thresholds for the Tm-doped fiber under investigation [7].

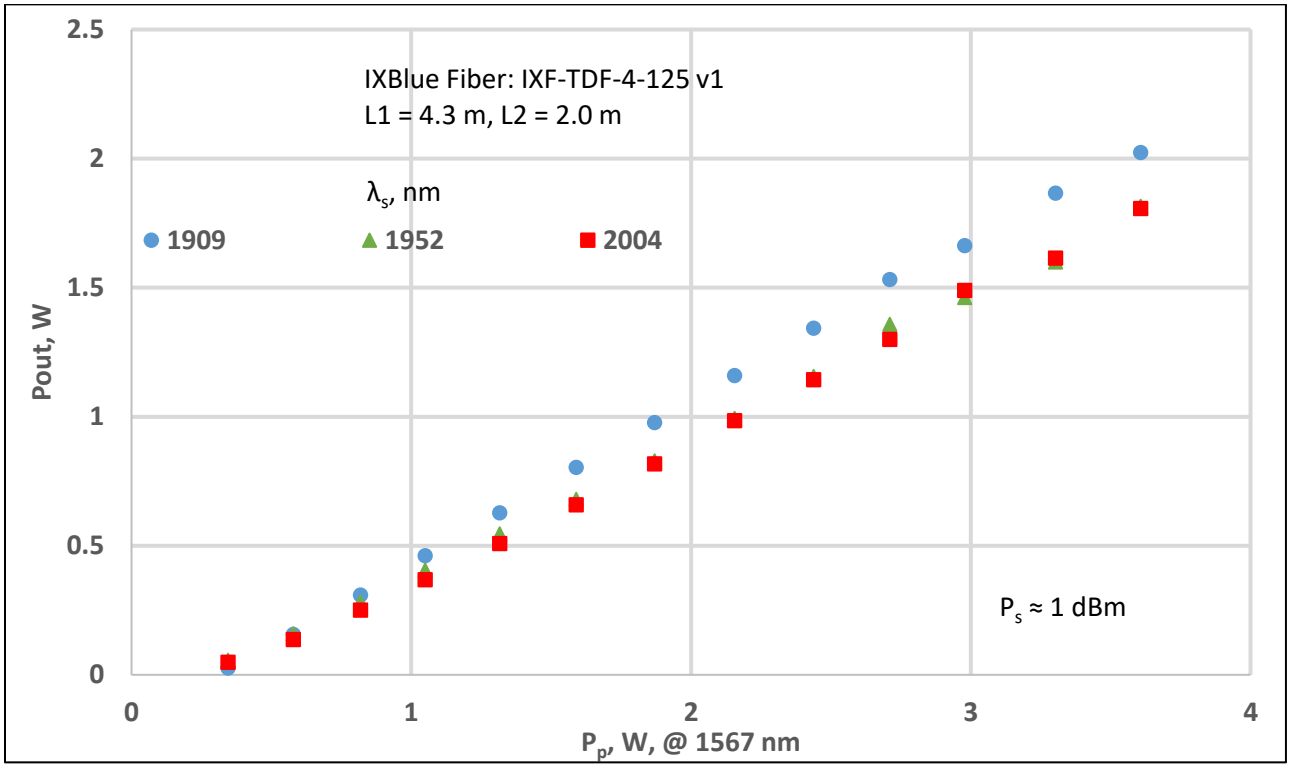

Figure 5. P_{out} vs. P_p with the Parameter of λ_s, for $P_s \approx 1$ dBm.

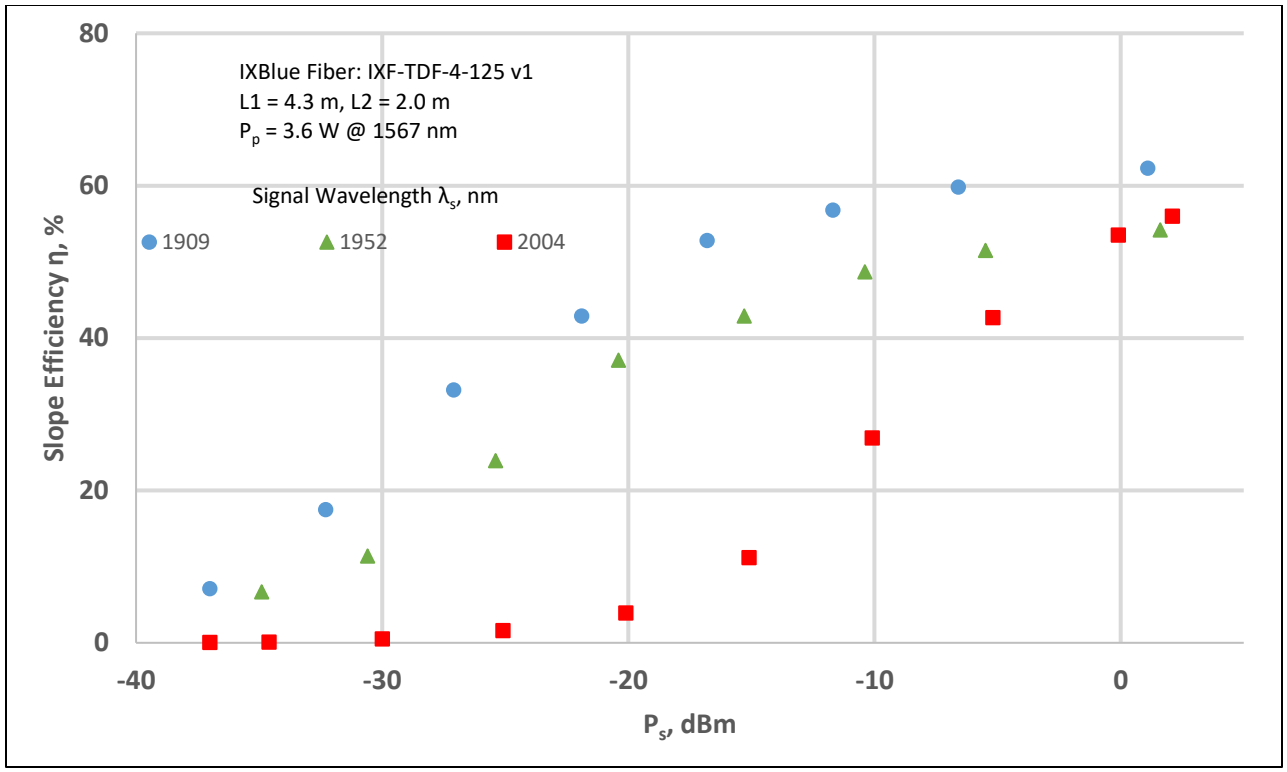

Figure 6. Slope Efficiency η vs. Signal Input Power P_s, with Signal Wavelength λ_s as Parameter.

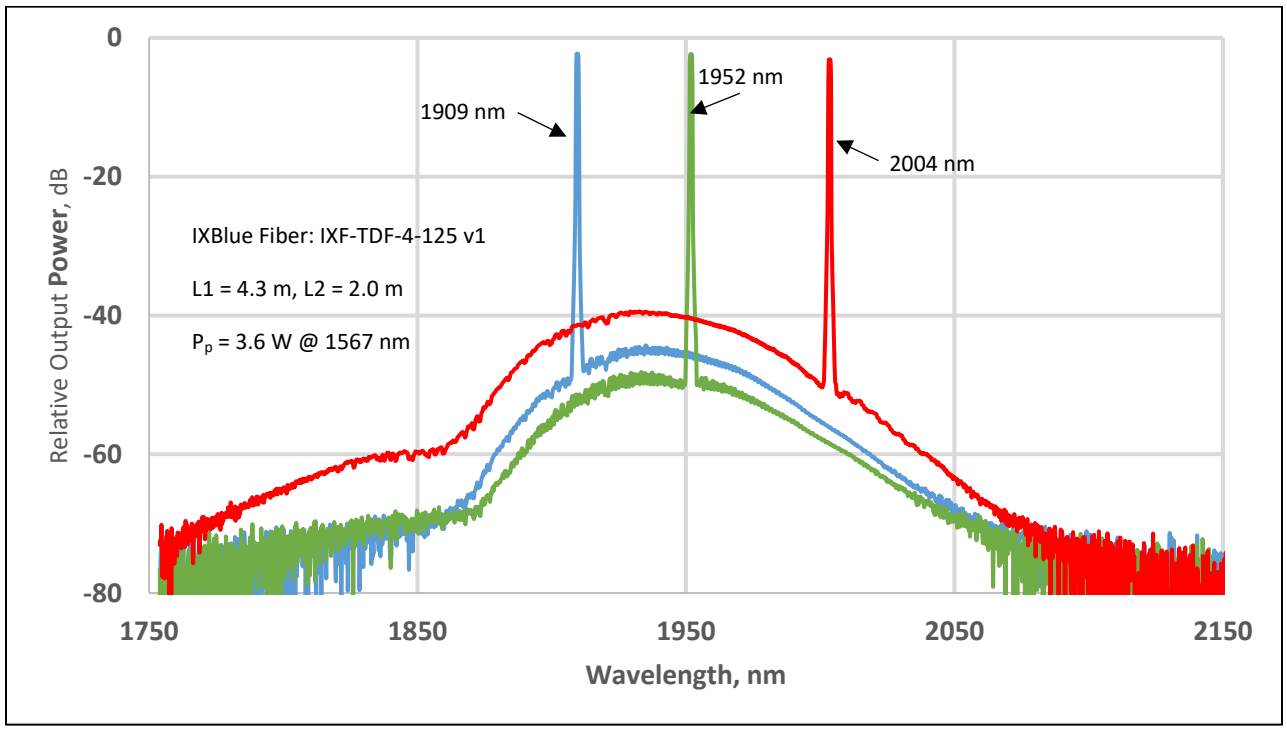

Figure 7. Saturated Output Spectra for the Tandem TDFA for Three Signal Wavelengths

The experimental saturated output spectra for three signal wavelengths of 1909, 1952, and 2004 nm are shown in Figure 7. Here P_{out} is approximately 2 W for each of the three curves. The evolution of the spontaneous emission background as a function of signal wavelength is quite interesting. As illustrated in Figure 7, the lowest spontaneous emission background occurs for λ_s = 1952 nm. The spontaneous background increases slightly for λ_s = 1909 nm, and then increases significantly for λ_s = 2004 nm. As with the behavior shown in Figure 6, this ASE variation is attributed to the change in amplifier saturation power as a function of wavelength. Taking the estimated value of the amplifier bandwidth from the points at which the ASE background is 15 dB down from the ASE peak, we can calculate BW = 139 nm for 1909 nm, 154 nm for 1952 nm, and 149 nm for 2004 nm. The average bandwidth obtained from these values yields an estimated TDFA BW of 147 nm.

Key experimental parameters for the two stage TDFA are summarized in Table 1 below. The largest observed difference is in the values of small signal gain as a function of signal wavelength, with a greatly decreased G for 2004 nm in comparison with 1909 and 1952 nm. All the other parameters measured are similar as a function of wavelength.

Experimental Parameter	**1909 nm**	**1952 nm**	**2004 nm**
Small Signal G, dB	60.4	56.9	41.6
Saturated P_{out}, W	2.02	1.81	1.82
Small Signal NF, dB	3.9	3.2	3.0
BW, nm	139	154	149
Dynamic Range, dB	37	37	37

Table 1. Key experimental parameters for the two-stage shared pump TDFA.

4. Comparison of Experiment with Simulation

We now compare the experimental performance of the tandem SC-TDFA with steady state simulations of amplifier behavior. The theory, methods, and physical parameters underpinning the simulations are presented in detail in Refs. [1-4, 8, 9].

Our first comparison of experiment and simulation is shown in Figure 8, which plots data for G and NF as a function of P_s for P_p = 3.61 W. Here we find that the simulated values of G for 1952 nm vary from the experimental data by less than 1 dB. For 1909 nm, the simulation predicts values of small signal gain that are about 3 dB larger than experiment, and for 2004 nm the simulated values of small signal gain are about 3 dB smaller than experiment. The origin of these differences as a function of wavelength is under investigation. Even though some differences are observed, the general trends of the gain simulations follow the experimental data quite closely.

The simulated noise figures agree with the experimental data to within 2 dB for λ_s = 1909 nm, and to within 1 dB for 1952 and 2004 nm. Again, the general trends of the simulations of NF follow the experimental values closely.

We next move to a comparison of P_{out} as a function of P_p for the three signal wavelengths. In this graph, the input signal power $P_s \approx 1$ dBm. For this case, the simulations predict slightly larger output powers than the experiments for all three wavelengths studied. For 1909 nm, the simulation predicts values 1.0 dB larger than experiment; for 1952 nm the difference is 0.8 dB; and for 2004 nm it is 0.4 dB. Similar differences have been

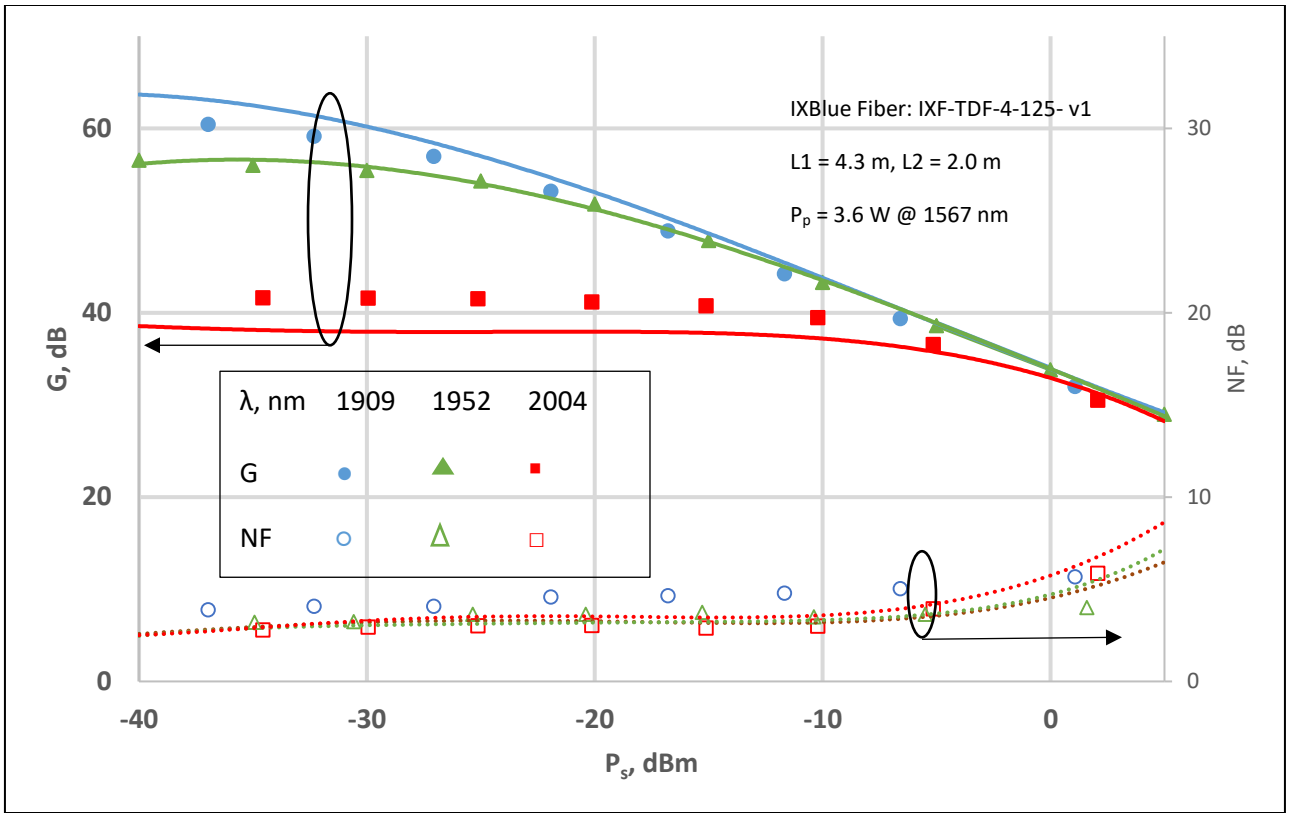

Figure 8. G and NF vs. P_s, with λ_s as the Parameter. Points: data. Lines: simulations.

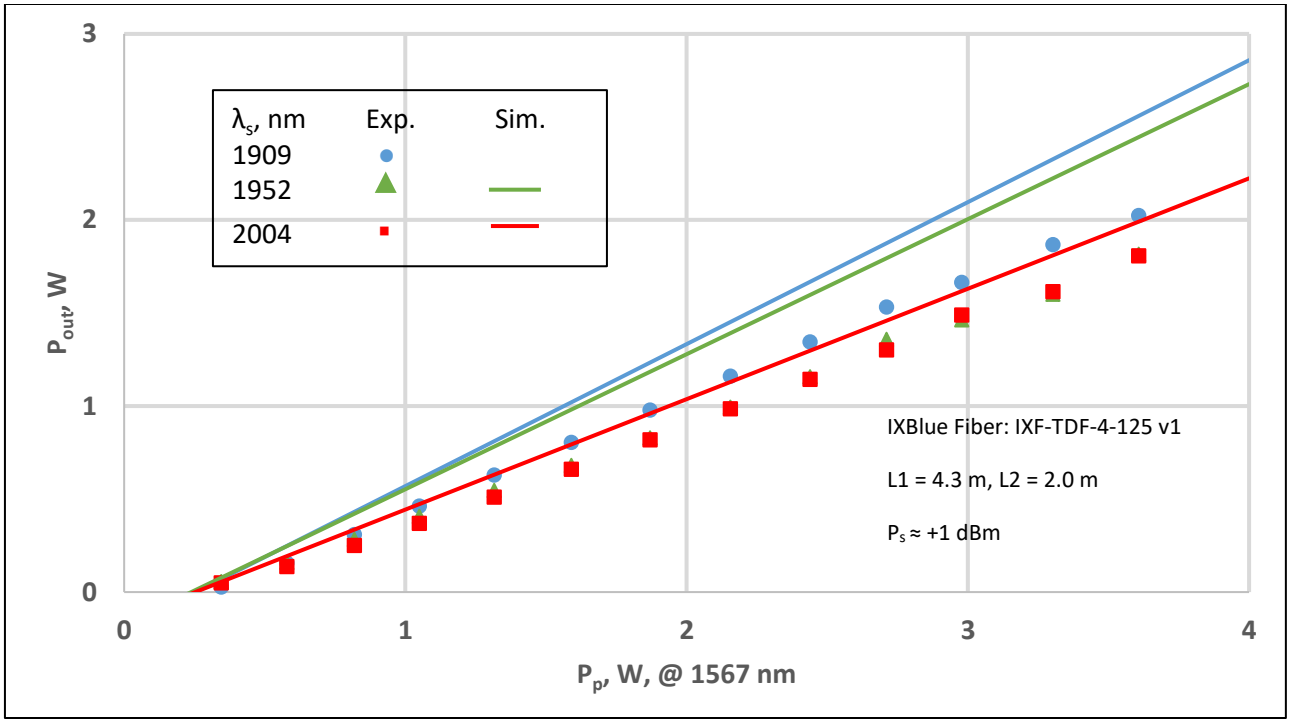

Figure 9. P_{out} vs. P_p with λ_s as the Parameter. Points: data. Solid lines: simulations.

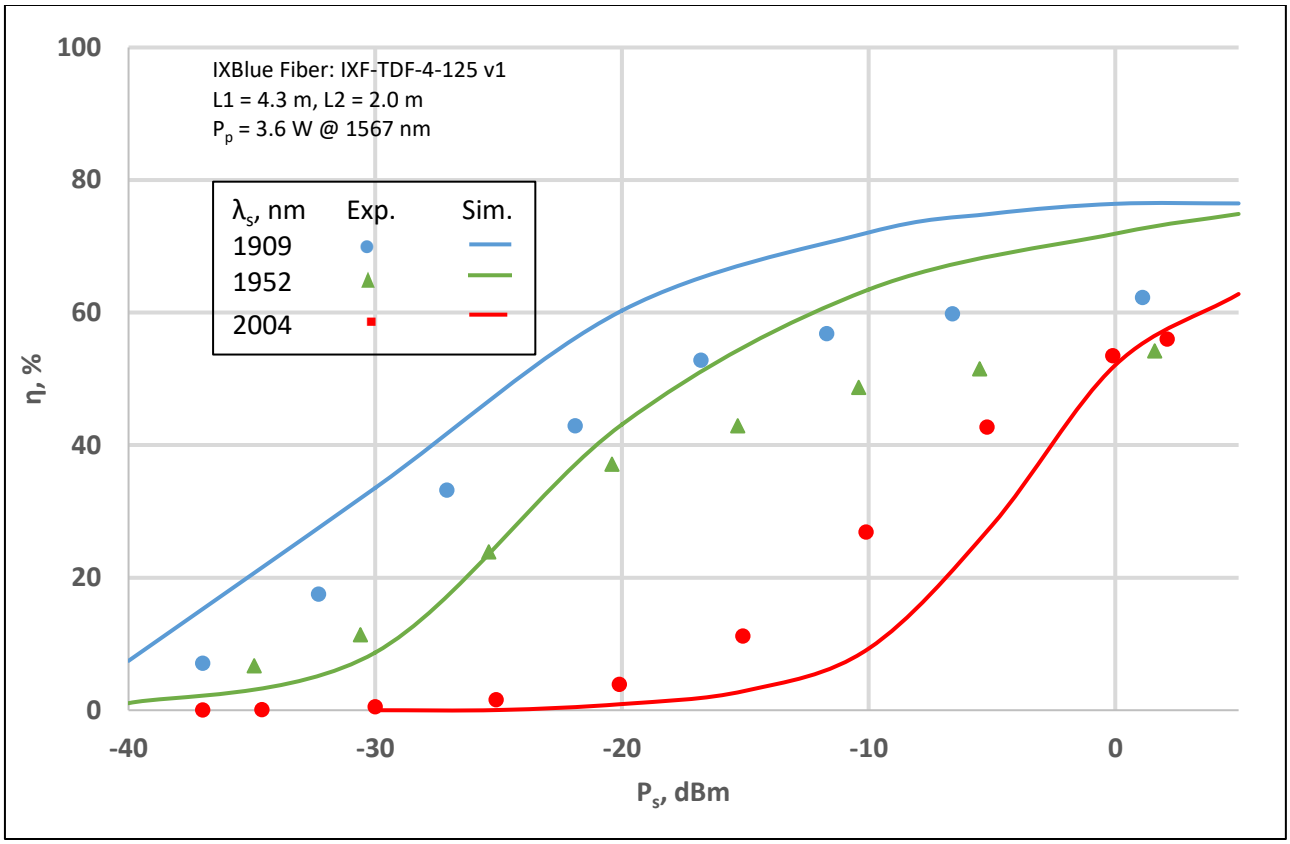

Figure 10. η vs. P_s with λ_s as the Parameter, Points: data. Lines: simulations.

observed in previous experimental and theoretical reports [2-4]. While the differences are measurable, we note that the simulations still yield saturated output power values within 1.0 dB of the data for all wavelengths studied. This relatively small difference indicates that the simulations are a powerful tool for designing multistage SC TDFAs.

By measuring P_{out} as a function of P_s and P_p, we next derived curves showing the variations in η as a function of P_s for the three signal wavelengths studied. Plots of η vs. P_s are shown in Figure 10. As with the gain curves in Figure 8, we see that the general trends of the data are predicted well by the simulations. In this case, the theory predicts larger values of η, relative to experiment, for 1909 and 1952 nm. Smaller values of η are predicted for 2004 nm. Maximum predicted slope efficiencies are in the range of 63 – 76.5 %, while maximum measured slope efficiencies fall within the range of 56 – 62 %. This agreement is consistent with the differences observed between theory and experiment in the saturated output power values plotted in Figure 9.

Another comparison of experiment and theory is given in Figure 11, where measured and simulated values of η are plotted as a function of λ_s for two representative values of P_s (+1 and – 20 dBm). As in Figure 10, the trend is for predicted values of η to be larger than the measured values. Nevertheless, we find that the trend of the simulated values is similar to experiment. From this plot, it is clear that the operating bandwidth of the amplifier is quite sensitive to the input power level. As in Ref. [4], simulated BW values for the amplifier can be derived from the points at which the theoretical curves cross a threshold of η = 50%. For + 1 dBm, the BW is found to be > 160 nm, while for -20 dBm it is 70 nm. The significant difference in BW as a function of P_s must be taken into account when designing preamplifiers which typically operate with $P_s \approx$ -15 to -30 dBm.

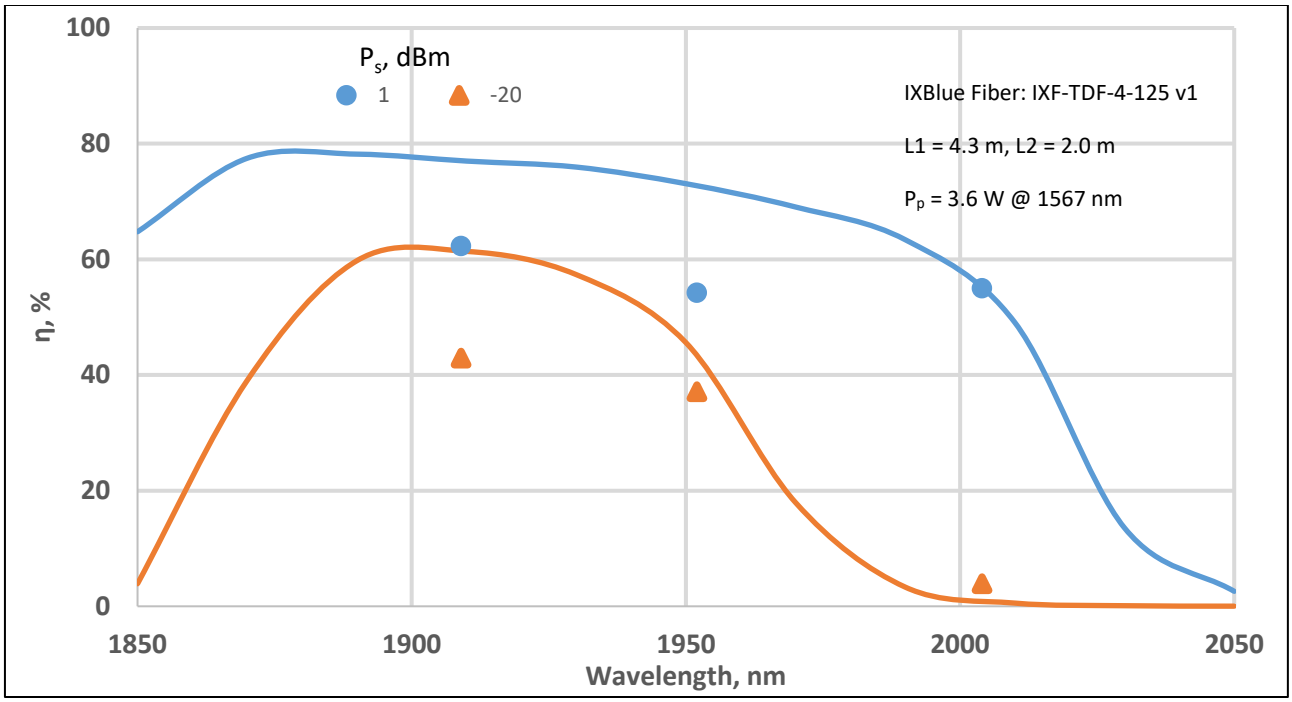

Figure 11. Slope Efficiency η as a Function of λ_s. Points: data. Solid lines: Simulations.

5. Comparison of Tandem Shared Pump TDFA with Single- and Multi-Stage Amplifier Performance

In Sections 3 and 4, we have shown that the shared pump tandem topology can deliver high performance that is fully in agreement with simulation results. Here we will compare the shared pump amplifier with a single stage, shared pump TDFA [4]. Summary performance of the two amplifiers is given below in Table 2.

			TDFA Configurations λ_s = 1952 nm	
Parameter	**Symbol**	**Units**	**1 Stage, Shared Pump**	**2 Stage, Shared Pump**
Pump Power (1567 nm)	**P_p**	W	3.2	3.6
Saturated Output Power	**P_{out}**	W	1.9	1.8
Small Signal Noise Figure	**NF**	dB	3.4	3.2
Signal Dynamic Range	**P_{in}**	dB	32	37
Small Signal Gain	**G**	dB	51	57
Slope Efficiency (Saturated)	**η**	%	66	54
Operating Bandwidth	**BW**	nm	167 (simulated)	147 (est. from ASE) >160 (simulated)

Table 2. Comparison of the Performance of TDFAs with Different Configurations

The table reveals that there are some significant differences in performance between the two TDFAs, and some similarities.

Comparing the maximum saturated output powers, we see that the one stage shared pump TDFA achieves 1.9

W output for 3.2 W available pump, while the two-stage shared pump amplifier achieves 1.8 W for 3.6 W of available pump. The optical-optical power conversion efficiencies are then 59.4% for the one stage configuration and 50.0 % for the two-stage configuration. A similar difference is apparent in the measured values of η, which are 66% for the one stage and 54% for the two stages. This difference in optical-optical power conversion efficiency and in η is caused by the insertion loss of isolator I2 which is present in the two-stage design but not in the one stage amplifier.

While the presence of I2 decreases η for the two stage TDFA, it nevertheless enhances the overall performance of this configuration, especially for the parameter of small signal gain G. Table 2 shows that the maximum small signal gain achieved with the one stage design is 51 dB, while 57 dB can be achieved with the two-stage configuration. We note that these is a similar increase in dynamic range from 32 dB for one stage to 37 dB for two stages. The presence of isolator I2 is responsible for the enhanced performance of the two-stage design because it suppresses self-lasing effects which appear for high values of pump power in the one stage TDFA. The enhanced values of G and dynamic range are very important for telecommunications applications such as in line repeaters and optical preamplifiers.

The minimum noise figures that are achieved with the two configurations are close to being equal, at 3.4 dB and 3.2 dB for one and two stages, respectively. These values are near the quantum limit of 3 dB, illustrating the high level of performance of our amplifier designs.

Table 2 shows that the operating bandwidth BW of the one stage amplifier is 167 nm (simulated) while for the two-stage amplifier it is 147 nm (estimated from the ASE background) and > 160 nm (derived from the simulation in Figure 11). We observe therefore that the bandwidths of the two configurations are approximately equal. Design techniques such as adjusting the lengths L1 and L2 of the two Tm-doped fibers in Figure 1 can be used to increase the operating bandwidth of the two-stage amplifier [4].

6. Discussion of Parameter Optimization for TDFA Architectures

The data reported in Figs. 2–11 illustrate several salient points about the operation of the shared pump TDFA.

From our experimental and theoretical studies here, and from the research reported in [4], it is evident that input power levels, saturated output power targets, noise figure specifications, small signal gain specifications, and operating signal bandwidths all depend in an interrelated way on the amplifier architecture. Design of an optimized amplifier requires a careful balancing of all these performance targets for the available pump power and the fiber lengths L1 and L2.

For gain amplifiers, Fig. 3 shows that it is very important to consider the input signal power level when choosing an optimum amplifier design. For example, at the coupling ratio of 30/70% and λ_s = 1952 nm, the fiber gain for −35 dBm input is highest at 57 dB for a pump power of 3.6 W. For −20 dBm input, the optimum gain is 51 dB; for -10 dBm input it is 42 dB; and for +1.6 dBm input it is 31 dB. Clearly the design specifications of the TDFA must be carefully considered when choosing an optimum P_s for a preamplifier designed to operate at low signal input powers.

Also for gain amplifiers, the G and NF values plotted for a pump power of 3.6 W in Figure 4 show that signal wavelength is exceedingly important in establishing gain specifications as a function of λ_s. The minimum small signal gain of 42 dB is observed at λ_s = 2004 nm, which is approaching the long wavelength boundary of the useful TDFA gain spectrum. This value is almost 20 dB smaller than the maximum observed gain of 60.4 dB at 1909 nm. While this variation must be taken into account, it should be noted that a gain of 40 dB or larger is usually sufficient for successful operation of an optical preamplifier for receivers in lightwave transmission systems. The NF values shown in Figure 4 vary only slightly with λ_s and P_s. These small variations are highly desirable in a TDFA design and demonstrate the high level of performance and robust nature of our two-stage

shared pump amplifier.

For power amplifiers, the data in Figure 2 show that high output power well in excess of 1 W can be obtained at λ_s = 1952 nm for P_s as low as -15 dBm. For $P_s \approx$1 dBm, output powers close or equal to 2 W are achieved for all three signal wavelengths of 1909, 1952, and 2004 nm as illustrated by the data in Figure 5. The measured output powers scale linearly with P_p up to the maximum pump power used of 3.6 W. This demonstrates the high performance achieved with our two-stage design.

No stimulated Brillouin scattering or other nonlinear effects were observed in our experiments. This means that we can improve the output power of the amplifier simply by increasing the pump power, up to the limit where nonlinear effects start to be observed. The threshold for SBS in our shared pump two stage amplifier is currently under study, and is initially estimated to be on the order of $P_{out} \approx$12-15 W [7].

Also for power amplifiers, variations in η as a function of P_s are illustrated in Figure 10 for both experimental data and for simulations. Here we see that the saturation behavior of the amplifier is quite different near the high wavelength boundary (2004 nm) of the Thulium-doped fiber gain spectrum, relative to performance at the center of the spectral band (1952 nm) and near the low wavelength boundary (1909 nm). This variation with P_s must be considered carefully in the design of wide BW power amplifiers.

For generic or multipurpose amplifiers, such as in-line amplifiers, Figure 7 shows quite interesting variations in the background amplified spontaneous emission (ASE) as a function of λ_s. As discussed in Section 3, we believe the variation in ASE levels is caused by variations in the saturation power of the amplifier with λ_s. This ASE background must be carefully considered when designing in-line repeaters for concatenated lightwave systems in the 2 μm region.

To conclude, we have shown that active fiber lengths L1 = 4.4 m and L2 = 2m, together with a pump coupling ratio of 30% co-pumping and 70% counter-pumping, provide balanced performance over a wide range of operating parameters for the two-stage shared pump TDFA configuration.

7. Summary

We have reported the experimental and simulated performance of a tandem SC TDFA with a shared in-band pump at 1567 nm. We measured and simulated the performance of the TDFA for parameters such as signal wavelength band, saturated output power, noise figure, small signal gain, and dynamic range. Our measurements and simulations show that the simulated operating bandwidth of the amplifier can be wider than 160 nm. We achieved saturated output powers of 2 W, small signal gains as high as 60.4 dB, noise figures as low as 3.2 dB, and a dynamic range of 37 dB for a noise figure of less than 5.6 dB. In all cases we found good agreement between our simulation tool and the experiments. No Brillouin scattering or other nonlinear effects were observed in any of our measurements.

Our experiments and simulations show that the two-stage shared pump TDFA can largely match the performance of the single stage shared pump amplifier reported in [4]. In addition, the two-stage amplifier has several advantages over the single stage design.

First, the presence of an interstage isolator prevents self-lasing both for small input powers (Ps ≈-30 dBm) and for signal wavelengths λ_s of 1909 and 2004 nm which are approaching the upper and lower edges of the useful Thulium gain band. Second, the interstage isolator improves the dynamic range of the two-stage amplifier by 6 dB in comparison to the single stage TDFA, by preventing self lasing and also by blocking backward ASE from the second stage. And third, the minimum observed noise figure of 3.2 dB for the two-stage amplifier is slightly better than the value of 3.4 dB obtained with the single stage design.

While the two-stage design is somewhat more complex than the one stage configuration, it nevertheless yields better performance in the three areas discussed above.

Finally, we observe that increasing the pump power slightly for the two-stage shared pump TDFA will compensate for the lower value of η in comparison to the one stage design. We also note that the operating BW of the two-stage amplifier can be increased by adjusting the lengths L1 and L2 of the active Thulium-doped fibers [4].

Taken together, the significant advantages we have demonstrated for the two-stage shared pump TDFA open the possibility for new and efficient 2 µm optical amplifiers for lightwave transmission systems as preamplifiers, as wideband in-line amplifiers, and as wideband power booster amplifiers.

8. Acknowledgments

We thank IXBlue Photonics for the single clad Tm-doped fibers, and Eblana Photonics for the single frequency discrete mode lasers in the 2000 nm band.

9. References

[1] C. Romano, R. E. Tench, Y. Jaouen, and G. Williams, "Simulation and design of a multistage 10 W thulium-doped double clad silica fiber amplifier at 2050 nm," in Proc. SPIE **10083**, Fiber Lasers XIV: Technology and Systems, 100830H (February 22, 2017). https://doi.org/10.1117/12.2250970

[2] R. E. Tench, C. Romano, and J.-M. Delavaux, "Broadband 2 W Output Power Tandem Thulium-doped Single Clad Fiber Amplifier at 2µm," IEEE Photonics Technology Letters **30** (5), 503-506 (2018). http://ieeexplore.ieee.org/document/8281047/

[3] C. Romano, R. E. Tench, Y. Jaouen, and J.-M. Delavaux, "Characterization of the 3F4 – 3H6 Transition in Thulium-doped Silica Fibres and Simulation of a 2µm Single Clad Amplifier," Paper P1.SC1.2, ECOC 2017, Gothenburg, Sweden. https://hal.archives-ouvertes.fr/hal-01663260/document

[4] R. E. Tench, C. Romano, and J.-M. Delavaux, "Optimized design and performance of a shared pump single clad 2 µm TDFA," Optical Fiber Technology 42, 18-23 (2018). https://doi.org/10.1016/j.yofte.2018.02.012

[5] E. Desurvire, "Erbium-Doped Fiber Amplifiers: Principles and Applications", New York, Wiley Interscience (1994).

[6] D. M. Baney, P. Gallion, and R. S. Tucker, "Theory and Measurement Techniques for the Noise Figure of Optical Amplifiers," Optical Fiber Technology **6**, 122-154 (2000). https://doi.org/10.1006/ofte.2000.0327

[7] A. Sincore, N. Bodnar, J. Bradford, A. Abdulfattah, L. Shah, and M. C. Richardson, "SBS Threshold Dependence on Pulse Duration in a 2053 nm Single-Mode Fiber Amplifier," J. Lightwave Technology **35**, 4000-4003 (2017). https://doi.org/10.1109/JLT.2017.2729508

[8] S. D. Jackson and T. A. King, "Theoretical modeling of Tm-doped silica fiber lasers," J. Lightwave Technology **17**, no. 5, pp. 948–956, May 1999. http://ieeexplore.ieee.org/document/762916/

[9] M. Gorjan, T. North, and M. Rochette, "Model of the amplified spontaneous emission generation in thulium-doped silica fibers," J. Opt. Soc. Am. B, 2886-2890 (2012). https://doi.org/10.1364/JOSAB.29.002886